Improved Analysis of Nonreciprocal Remanence Ferrite Phase Shifter in Grooved Waveguide

Wenquan Che, Edward Kai-Ning Yung, *Senior Member, IEEE,* Suibing Chen, and Junding Wen

***Abstract*—In this paper, the nodal finite-element method is used to analyze the differential phase shift of a nonreciprocal remanence ferrite phase shifter in a grooved waveguide. Instead of the former twin-slab model, an improved analytical model is adopted, where the effect of every part of a ferrite toroid on the differential phase shift has been considered. This analysis may replace the correcting factor with good agreement with the experimental data. Furthermore, this analysis is employed to investigate the effect of corner chamfering on the figure-of-merit (differential phase shift per decibel insertion loss) of a ferrite phase shifter. The numerical results are found to agree with the experiments in the literatures.**

***Index Terms*—FEM, ferrite toroid corner chamfering, grooved waveguide, improved analysis, nonreciprocal remanence ferrite phase shifter.**

I. Introduction

THE nonreciprocal remanence ferrite phase shifter, as a beam-steering element in phased array radars, has found its applications extensively because of its remarkable performances [1]. Many techniques for improving the characteristics have been developed. In order to optimize the figure-of-merit, Ince and Stern [2] suggested a new idea of dielectric rib insertion in the slot of a ferrite toroid, which has yielded improvement on the figure-of-merit markedly. In 1968, Clark [3] proposed a new technique of toroid corner chamfering to increase the figure-of-merit by approximately 20%. This improvement has been obtained with apparently no degradation of other phase-shifter parameters, except possibly in average power capability. In 1971, Ince *et al.* [4] also investigated the effect of toroid corner chamfering on the differential phase shift, and the experimental results were proven to improve the figure-of-merit of the phase shifter by approximately 10%. Successively, Junding [5] and Mizobuchi and Kurebayashi [6] presented a new configuration of the nonreciprocal remanence ferrite phase shifter in a grooved waveguide, which significantly improves the figure-of-merit, average power-handling ability, peak power-handling capability, etc. In the 1990s, different improvement techniques [7], [8] on the nonreciprocal remanence ferrite phase shifter have been proposed. Due to the complex boundary conditions, in the above-mentioned literature, the toroidal phase shifters in a rectangular or grooved waveguide have been approximated by the twin-slab configuration, and analyzed with theoretical methods by Lax and Button [9] and by Schlomann [10], where the ferrite toroid has been replaced by two oppositely magnetized slabs that extend over the complete height of the waveguide. However, the analytical methods based on a twin-slab model did not consider the magnetization at the ferrite corners, which resulted in the discrepancy between the experimental and theoretical results. Although the correcting factor [2] could be employed to modify the calculation results, the discrepancy between theoretical results and measured data also cannot be negligible. In addition, there has not been a helpful correcting factor used to modify the theoretical differential phase shift in grooved waveguide. Therefore, an improved analysis of the differential phase shift in a grooved waveguide by the finite-element method (FEM) [11], [12] has been carried out in this paper. Firstly, we analyzed the effect of the magnetization or nonmagnetization of the center ferrite of the toroid on the differential phase shift, and we found that they could be regarded as dielectric. Secondly, we continued to analyze the effect of magnetization or nonmagnetization of the four small triangular corner of the ferrite toroid, and we have obtained the same conclusion. Finally, an improved analytical model has been given and the numerical calculation of the differential phase shift has been carried out. Compared with theoretical results obtained from the twin-slab model and then multiplied with a correcting factor, the numerical results have been found to agree better with the measured data. Moreover, to the best of our knowledge, there has been little literature published to analyze theoretically the effect of the toroid corner chamfering on the performance of the ferrite phase shifter. Hence, the improved analysis based on the FEM has also been employed to analyze this problem, and the numerical results have been found to agree with the measured data in the literature.

Manuscript received May 9, 2001. This work was supported by the Research Grant Council under Competitive Earmarked Research Grant, HKSAR under Project: 9040456(CityU 1200/99E).

W. Che is with the Department of Electronic Engineering, City University of Hong Kong, Kowloon, Hong Kong and is also with the Department of Electrical Engineering, Nanjing University of Science and Technology, Nanjing, China.

E. K.-N. Yung is with the Department of Electronic Engineering, City University of Hong Kong, Kowloon, Hong Kong.

S. Chen is with the Department of Antenna and Feeding, East China Institute of Electronic Engineering, Hefei, China.

J. Wen is with the Department of Electrical Engineering, Nanjing University of Science and Technology, Nanjing, China.

Publisher Item Identifier 10.1109/TMTT.2002.801331.

II. Improved Analysis of the Ferrite Toroid Corners of Nonreciprocal Remanence Ferrite Phase Shifter

A. Consideration of the Effect of the Ferrite Located Near the Center in a Waveguide on the Differential Phase Shift

In order to analyze the differential phase-shift characteristic of the nonreciprocal remanence ferrite phase shifter in a grooved waveguide, we have carried out the following analysis. Firstly, as mentioned by Ince and Stern [2], if the ferrite near the center of the rectangular waveguide is replaced with a dielectric rib,

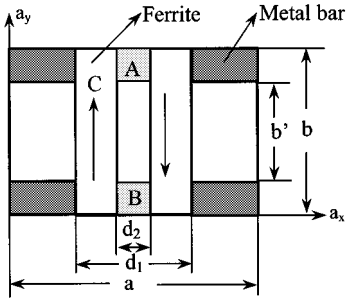

Fig. 1. Model used to analyze the effect of the ferrite near the center of the waveguide.

having same dielectric constant as the ferrite, the maximum phase shift remains the same. In other words, this suggests that the magnetization of the ferrite near the center of the waveguide contributes little to the differential phase shift. Of course, because the transverse RF magnetic field vector in this region is parallel to magnetization, the interaction of the ferrite with the electromagnetic field is the same, as with the dielectric; therefore, the field-displacement effect responsible for phase shift does not occur in this part of the ferrite toroid. The analysis model is depicted in Fig. 1(a) with coordinate axes. Due to symmetry, the plane $x = a/2$ is equivalent to a perfect magnetic conductor for the dominant quasi-TE_{10} mode, allowing to restrict the calculations to one-half of the waveguide cross section.

In this paper, the nodal element FEM has been employed. The magnetic vector and electric scalar potentials have been introduced in this method, which is proven to be very beneficial to eliminating a large number of spurious modes [11], [12]. The finite-element equation is expressed as

$$\left\{\begin{bmatrix}[M_{AA}] & [0]\\ [0] & [0]\end{bmatrix} - K_0^2\begin{bmatrix}[N_{AA}] & [N_{AV}]\\ [N_{VA}] & [N_{VV}]\end{bmatrix}\right\}\begin{bmatrix}A\\ V\end{bmatrix} = 0 \quad (1)$$

where $[M]$ and $[N]$ are symmetric and sparse matrices; A is the vector magnetic potential and V is the scalar electric potential. The boundary conditions to be applied are listed as follows.

1) On electric walls

$$\vec{A}\times\vec{n} = 0 \quad (2)$$
$$V = 0 \quad (3)$$
$$\nabla\cdot\vec{A} = 0. \quad (4)$$

2) On magnetic walls

$$\nabla\times\vec{A}\times\vec{n} = 0 \quad (5)$$
$$(\vec{A}+\nabla V)\cdot\vec{n} = 0 \quad (6)$$
$$\vec{A}\cdot\vec{n} = 0. \quad (7)$$

Of which, (4)–(6) are the natural boundary conditions and (2), (3), and (7) are the Dirichlet boundary conditions. For the practical geometry illustrated in Fig. 1, the expressions of the matrices $[M]$ and $[N]$ in (1) are given in Appendix.

It should be noted, as indicated by Green and Sandy [13] and Schlomann [14], if one is concerned with ferrite phase shifters, then the microwave characterization of the ferrite material should describe the partially magnetized state of the ferrite. In this case, assuming that the magnetization is located in the x–y-plane, making an angle θ with the $\bar{a}_Y$ coordinate axis. In the x, y, and z systems, the relatively permeability tensor of the ferrite is then given by

$$\begin{aligned}[\mu_r] &= \begin{bmatrix}\cos\theta & -\sin\theta & 0\\ \sin\theta & \cos\theta & 0\\ 0 & 0 & 1\end{bmatrix}\begin{bmatrix}\mu & 0 & -jk\\ 0 & \mu_Y & 0\\ jk & 0 & \mu\end{bmatrix}\\ &\quad\cdot\begin{bmatrix}\cos\theta & \sin\theta & 0\\ -\sin\theta & \cos\theta & 0\\ 0 & 0 & 1\end{bmatrix}\\ &= \begin{bmatrix}\mu\cos^2\theta+\mu_Y\sin^2\theta & (\mu-\mu_Y)\cos\theta\sin\theta & -jk\cos\theta\\ (\mu-\mu_Y)\cos\theta\sin\theta & \mu\sin^2\theta+\mu_Y\cos^2\theta & -jk\sin\theta\\ jk\cos\theta & jk\sin\theta & \mu\end{bmatrix}\end{aligned} \quad (8)$$

where [13]

$$\begin{aligned}\mu &= \mu_d + (1-\mu_d)\left\{\frac{M}{M_S}\right\}^{3/2}\\ \mu_Y &= \mu_d\left(1-(M/M)_S\right)^{5/2}\\ \mu_d &= \frac{2}{3}\left[1-\left(\frac{\gamma 4\pi M_S}{\omega}\right)^2\right]^{1/2}+\frac{1}{3}\\ k &= \gamma 4\pi M/\omega.\end{aligned} \quad (9)$$

Gyromagnetic ratio $\gamma = 2.8\times 10^6$ Hz/Oe, remanence ratio $R = 4\pi M/4\pi M_S$, $4\pi M_S$ is the saturated magnetization of the ferrite, $4\pi M$ is the remanence magnetization of the ferrite, and ω is the operating frequency. At first, we consider the magnetization of the ferrite located near the center of the ferrite toroid, which is denoted as A and B in Fig. 1. In this case, the relative tensor permeability of the ferrites A and B are given as (A1) and (A2) in the Appendix. The parameters used in the calculation are listed as follows: $4\pi M_S = 2200$ Gs $R = 0.85$, $\varepsilon_f = 13.0$, $a = 0.4928\lambda_0$, $b = 0.2144\lambda_0$, $b' = 0.1568\lambda_0$, $d_1 = 0.1312\lambda_0$, $d_2 = 0.0192\lambda_0$; the calculation results are shown as solid lines in Fig. 2. In addition, we replace the ferrites in regions A and B with dielectrics, and the differential phase shift calculated by the FEM is also depicted as dotted lines in Fig. 2, which is approximately the same as that in the case of considering the magnetization of ferrites in regions A and B. Therefore, in the following analysis, we will regard the ferrites in regions A and B as dielectric, having the same dielectric constant with the ferrite material. It should be noted that the results were not multiplied with a correcting factor.

B. Consideration of the Effect of Ferrite Toroid Corners on Differential Phase Shift

The analytical model in Fig. 3(a) illustrates the slightly exact magnetization of the ferrite toroid. In any case, the magnetization in the corners of the toroid with area $w\times w$, denoted as C_1, C_2, C_3, and C_4, does not lie normal to the direction of the microwave field and, hence, the ferrites in the corners contribute less to differential phase shift than other ferrites do. Therefore, the twin-slab model used in the literature is not suitable for the

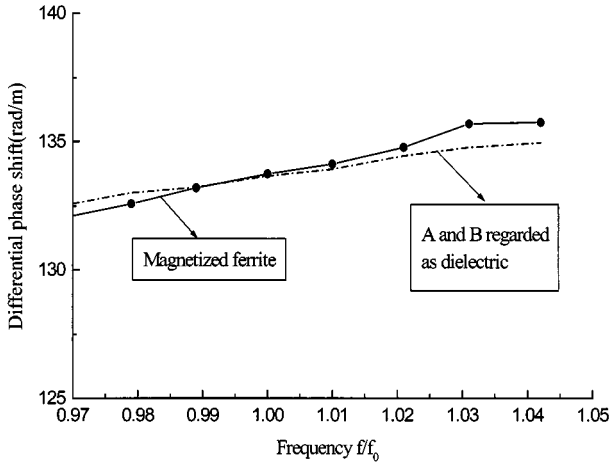

Fig. 2. Effect of the ferrite near the center of the ferrite toroid in the grooved waveguide on the differential phase shift (not multiplied with the correcting factor).

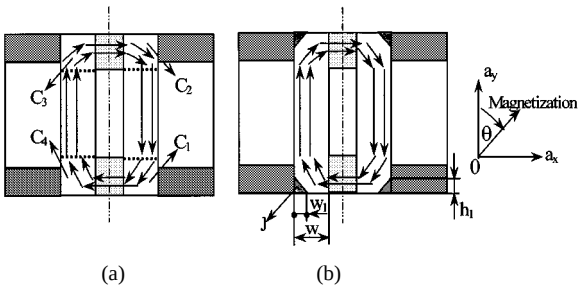

(a) (b)

Fig. 3. (a) Practical magnetization in the ferrite toroid of the latching ferrite phase shifter in grooved waveguide. (b) The model employed to analyze the effect of the four small orthogonal triangles on the differential phase shift.

accurate analysis of the differential phase shift of ferrite phase shifter. In the following section, instead of a twin-slab model, we first select the angles θ between the magnetization in four corners of the ferrite toroid as $|45°|$ and then analyze the differential phase-shift characteristic of the device. In succession, the effect of four triangular corners denoted as J in Fig. 3(b) has also been considered, and we found that they could be regarded as dielectric.

1) Effect of the Four Square Corners of the Ferrite Toroid on the Differential Phase Shift ($\theta = |45°|$): Firstly, in the four square corners of the ferrite toroid C_1, C_2, C_3, and C_4, the angles θ between the magnetization and $\vec{a}_Y$ axis are chosen as 45°, −45°, 45°, and −45°, respectively, and the calculated differential phase shift has been shown as the solid line of Fig. 4, with the measured data of a practical prototype. It is not hard to see, after considering the practical magnetization of the four square corners in the toroid ($\theta = |45°|$), though the discrepancy between the calculated and measured differential phase shift is as large as approximately 11%, the trend of frequency characteristic is approaching the experimental results. Without any doubt, this is owing to the rough treatment on the magnetization in the four square corners of the ferrite toroid.

2) Consideration of the Magnetization of the Four Orthogonal Triangular Corners of the Ferrite Toroid on the Differential Phase Shift: Furthermore, the four small orthogonal triangular corners in the ferrite toroid, denoted as J in Fig. 3(b), are a little

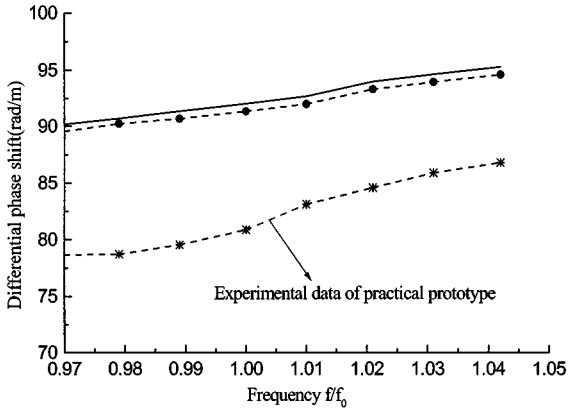

Fig. 4. Comparison of the numerical differential phase shifts (when $\theta = |45°|$ at the four square corners) with measured data of one practical prototype. Solid line: the angles between magnetization and the $\vec{a}_Y$ axis θ equal to $|45°|$ at the four square corner. Line with circle: ferrites in four orthogonal triangular corners ($w_1 = h_1 = (1/4)w$) considered as dielectric.

far away from the center of the ferrite toroid, and the magnetization does not lie normally to the direction of the microwave field, which should have little contribution to the energy accumulation in the ferrite toroid. Hence, whether magnetization or nonmagnetization of the ferrite in this region should has little effect on the differential phase shift. In order to verify our estimation, we replaced the four small orthogonal triangular corners with dielectric having same dielectric constant as ferrite material, and differential dimension has been considered. The numerical results illustrated via the dotted line in Fig. 4 indicate that, when the four small orthogonal triangular corners have been regarded as dielectric, and their areas equal $1/2 \times w/4 \times w/4$, the differential phase shift remains approximately the same, and the maximum discrepancy is only 0.72%.

Therefore, in order to get more precise results, in the following section, we will present an improved analytical model, where the four square corners will be separated into several parts with different magnetization angles. In addition, we will regard ferrites A, B, and J as dielectrics, and will not consider their magnetization.

C. Improved Analysis of the Characteristic of the Differential Phase Shift of the Nonreciprocal Remanence Ferrite Phase Shifter

Based on above-mentioned analysis, the final analytical model is illustrated in Fig. 5; the ferrite toroid has been separated into C, M, N, O, P, and J, respectively. Note that the geometry is symmetrical, hence, only half of it has been analyzed. The ferrites in parts C and J can be regarded as dielectric, having same dielectric constant with the ferrite material. We only need to consider the magnetization in parts P, M, N, and O. The angle between the magnetization path in them and $\vec{a}_Y$ axis is 0°, 60°, 45°, and 30° respectively. The corresponding permeability tensors are expressed as (A3)–(A6) in the Appendix. The numerical results have been shown in Fig. 6, together with the experimental results of our practical prototype. It is noticed that, compared with the analytical results using a twin-slab model [5], [6], the numerical results obtained by the improved analysis agree better with

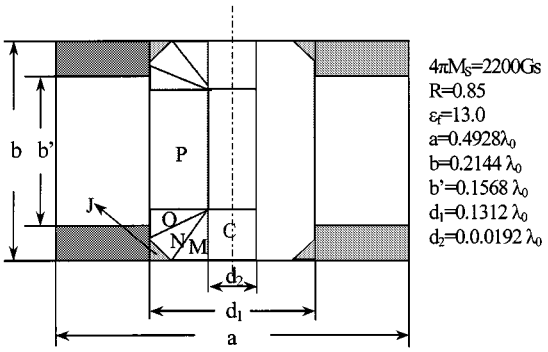

Fig. 5. Final analysis model employed to calculate the differential phase shift.

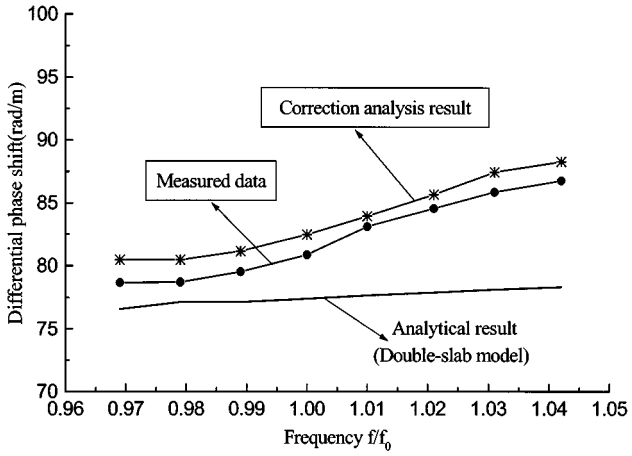

Fig. 6. Comparison of the differential phase shift among the improved analysis results, analytical results, and experimental data.

the measured data, the discrepancy is now only 3%; while the analytical results do not agree with the measured results, not only in the values, but in the trend of frequency characteristic. In addition, it must be mentioned that the analytical results were multiplied with the correcting factor $\alpha = 1 - (d_1 - d_2/b)$ [2]. Owing to the independence on frequencies, the correcting factor cannot reflect the change of the frequency characteristic of the differential phase shift; therefore, this kind of disposal is not satisfactory. In any case, in our improved analysis, we considered the magnetization in every part of the ferrite toroid in detail and, because the tensor permeability of the ferrite is the function of frequencies, the numerical results can approximately reflect the practical frequency characteristic of the differential phase shift of the device. There, of course, existed some discrepancy between the measured data and improved analysis results, partially because of the rough segment of the ferrite corner, if we can separate them into more parts, which can be a great help to obtain more accurate results agreeing well with the experimental data. On the other hand, an important possible source of discrepancy is the rather large spread of the remanent magnetization M_r, as this quantity appears to be very sensitive to small changes in the manufacturing process; and the incorrect measurement of dielectric constant ε_r also has some contribution to the discrepancy.

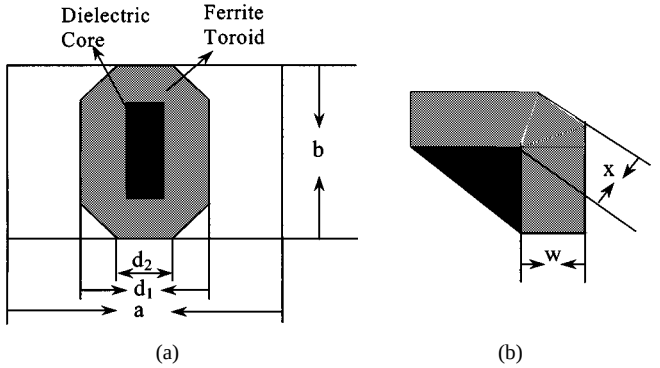

Fig. 7. (a) Cross section of latching ferrite phase shifter in the rectangular waveguide. (b) Details of ferrite toroid corner chamfer.

III. Numerical Analysis of Ferrite Toroid Corner Chamfering

A. Theoretical Analysis

Clark [3] has described the corner-chamfering technique for improving the figure-of-merit of nonreciprocal latching ferrite phase shifters. The configuration of interest illustrated in Fig. 7(a) is the cross section of the nonreciprocal remanence ferrite phase shifter in the rectangular waveguide. It was discovered by Clark [3] that the differential phase shift per unit length might be increased by chamfering the corners of the toroid in the manner depicted in Fig. 7(b), and the enhancement could reach its maximum value when $x/w = 1.0$, i.e., the chamfer angle equals 45°. Clark has also found that the figure-of-merit could be increased by approximately 20%; Ince *et al.* concluded in [4] that chamfering the phase-shifter toroid could yield a maximum increase in differential phase shift of approximately 10% for the constant phase design. There seems to exist some argument between their conclusions. However, up to now, no theoretical analysis has been found in the literatures to verify the validity of their proposals. Hence, the improved analysis based on the FEM previously discussed has also been employed to analyze this structure.

The parameters are given as follows: $f_0 = 3.3\,\text{GHz}, 4\pi M_S = 800$ Gs, the dielectric constant of the ferrite material is $\varepsilon_f = 14.8$, $a = 18.288$ mm, $b = 15.748$ mm, $d_1 = 8.89$ mm, $d_2 = 2.54$ mm, and the length of the ferrite toroid $l = 152.4$ mm. Several different types of dielectric core material have been adopted, having dielectric constants ranging from 16.0 to 100. The only consideration of choosing these dielectric constants is that we could compare our numerical results with the experimental data presented by Ince *et al.* [4].

For the purpose of simplicity, we first analyze the characteristic of differential phase shift of the ferrite phase shifter with corner chamfering using the twin-slab model. Based on the previous analysis, we regarded the center ferrites as dielectric, with a comparable dielectric constant as that of the ferrite. We originally believed that the numerical results would indicate an increase tendency of the differential phase shift. However, very surprisingly, the differential phase shift of the device with corner chamfering is actually smaller than the case without corner chamfering. Actually, the results were reasonably accurate. Since we did not consider the actual magnetization of the ferrite corners when we adopted the twin-slab model to carry

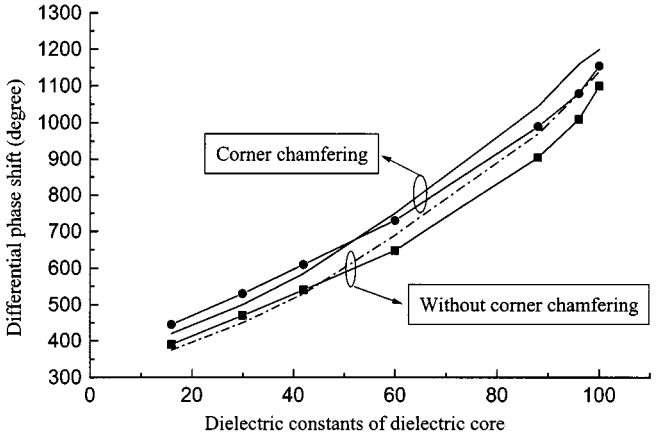

Fig. 8. Differential phase shift versus dielectric constant of the dielectric core. Lines with a symbol: our results. Lines without a symbol: Ince *et al.*'s experimental data.

out our analysis, every part of the ferrite toroid (except for the center ferrites) has been regarded as having the same contribution to the differential phase shift. Therefore, undoubtedly, the removal of the four corners shown in Fig. 7 should result in the decrease of ferrite volume having a contribution to the phase shift; accordingly, the decrease of the difference phase shift was inevitable and logical.

B. Comparison Between Numerical Results and Experimental Data

In order to analyze the practical effect of the toroid corner chamfering on the differential phase shift of the ferrite phase shifter, the improved analysis discussed in the previous section will be employed to analyze this issue. The numerical results have been depicted in Fig. 8, together with the experimental data of Ince *et al.* [4]. The improvement of differential phase shift resulting from the corner chamfering shows nearly the same trend with the experimental data proposed by Ince *et al.*, and the enhancement of the differential phase shift decrease along with the increase of the dielectric constants of the dielectric core. Obviously, when the dielectric constant goes beyond some of the values, the energy has been accumulated mainly in the center of the ferrite toroid; the removal of the four corners of the ferrite toroid should have less effect on the differential phase shift of the ferrite phase shifter; the small decrease of the ferrite could not affect the differential phase shift markedly.

From Fig. 8, we can see that, the maximum improvement of calculation results is 14.09%, and the experimental result of Ince *et al.* is 12%, occurring when $\varepsilon_r = 16.1$. In addition, the minimum improvement of calculation is 5%. The measured data is 5.26%, occurring when $\varepsilon_r = 100$; therefore, there has been an obvious discrepancy between them. The following reasons have been found to contribute to the observed difference.

1) The remanence ratio R has not been given in [4], thus, we can only select one by our experience.
2) During our improved analysis, the precision of magnetization simulation may not high enough.
3) An important possible source of discrepancy is the rather large spread of the remanent magnetization M_r, as this quantity appears to be very sensitive to small changes in the manufacturing process. The incorrect measurement of dielectric constant ε_r also has some contribution to the discrepancy.

Undoubtedly, the performance of rectangular toroid phase shifters can be somewhat improved by chamfering the corners; this increases the differential phase shift, while losses are slightly reduced due to removal of ferrite corners, therefore, the figure-of-merit could be improved significantly. However, it should be noted that this technique has also resulted in the degradation in average power capability of the nonreciprocal remanence ferrite phase shifter. From average power capability consideration alone, it is not advisable to adopt this technique to improve the performances of the device. However, in the case of low average power, ferrite corner chamfering is undoubtedly a good choice to improve the performances of the device.

IV. Conclusion

In this paper, the ferrite toroid corner improved analysis using a nodal FEM has been proposed to carry out the analysis of differential phase shift of a nonreciprocal remanence ferrite phase shifter in a grooved waveguide. During the analysis, an improved analytical model has been presented, where the magnetization of every part of the ferrite toroid has been taken into account in detail, and the different magnetization angles have been introduced in every parts of the ferrite toroid. The numerical results agree well with the experimental data of our practical prototype, which indicates that the improved analysis method could replace the traditional correcting factor. Owing to the independence on frequency, the correcting factor cannot reflect the actual frequency characteristic of the differential phase shift, thus resulting in the large discrepancy between analytical results and measured data. The theoretical analysis also indicated that the ferrite located near the center of the waveguide and the four small orthogonal triangular corners of the ferrite toroid could be treated as an dielectric, having a comparable dielectric constant with the ferrite material, i.e., it is not necessary to consider their magnetization when we analyze the differential phase shift of the device. In addition, the effect of toroid corner chamfering on the figure-of-merit of the nonreciprocal remanence ferrite phase shifter has been investigated, and the numerical results agree with the experiments in literature. This result supports that the differential phase-shift enhancement is due to a shaping of the RF field distribution in the vicinity of the chamfer, and the effect of the chamfer is to cause the electrical lines to bend in the vicinity of the chamfer and become more parallel to the remanent flux lines. From average power capability considerations alone, it is not advisable to adopt this technique to improve the performances of the device owing to the degradation in average power capability of the nonreciprocal remanence ferrite phase shifter resulting from the reduction of the area of contact between the toroid and the waveguide.

APPENDIX

The present finite-element formulation uses triangular elements. The matrix elements of $[M]$ and $[N]$ in (1) are given as follows:

$$[M_{11}^e] = \iint_e \left[P_{yy}\beta^2 (N_e)(N_e)^T + P_{zz}\frac{\partial (N_e)}{\partial y}\frac{\partial (N_e)^T}{\partial y} + \frac{1}{3}\frac{\partial (N_e)}{\partial x}\frac{\partial (N_e)^T}{\partial x}\right] dx\,dy$$

$$[M_{12}^e] = [M_{21}^e] = \iint_e \left[-P_{xz}\beta (N_e)^T \frac{\partial (N_e)}{\partial y} - P_{zz}\frac{\partial (N_e)}{\partial y}\frac{\partial (N_e)^T}{\partial x}\right] \cdot dx\,dy$$

$$[M_{13}^e] = [M_{31}^e] = \iint_e \left[P_{yy}\beta (N_e)\frac{\partial (N_e)^T}{\partial x} - P_{xz}\frac{\partial (N_e)}{\partial y}\frac{\partial (N_e)^T}{\partial y}\right] \cdot dx\,dy$$

$$[M_{22}^e] = \iint_e \left[P_{xx}\beta^2 (N_e)(N_e)^T + P_{xz}\beta (N_e)^T \frac{\partial (N_e)}{\partial x} + P_{xz}\beta (N_e)\frac{\partial (N_e)^T}{\partial x} + P_{zz}\frac{\partial (N_e)}{\partial x}\frac{\partial (N_e)^T}{\partial x} + \frac{1}{3}\frac{\partial (N_e)}{\partial y}\frac{\partial (N_e)^T}{\partial y}\right] dx\,dy$$

$$[M_{23}^e] = [M_{32}^e] = \iint_e \left[P_{xx}\beta (N_e)\frac{\partial (N_e)^T}{\partial y} + P_{xz}\frac{\partial (N_e)^T}{\partial y}\frac{\partial (N_e)}{\partial x}\right] \cdot dx\,dy$$

$$[M_{33}^e] = \iint_e \left[P_{xx}\frac{\partial (N_e)}{\partial y}\frac{\partial (N_e)^T}{\partial y} + P_{yy}\frac{\partial (N_e)}{\partial x}\frac{\partial (N_e)^T}{\partial x} + \frac{1}{3}\beta^2 (N_e)(N_e)^T\right] dx\,dy$$

$$[M_{14}^e] = [M_{24}^e] = [M_{34}^e] = [M_{41}^e] = [M_{42}^e] = [M_{43}^e] = [M_{44}^e] = 0$$

$$[N_{11}^e] = [N_{22}^e] = [N_{33}^e] = \iint_e \varepsilon_r (N_e)(N_e)^T\,dx\,dy,$$

$$[N_{14}^e] = [N_{41}^e]^T = \iint_e \varepsilon_r (N_e)\frac{\partial (N_e)^T}{\partial x}\,dx\,dy$$

$$[N_{24}^e] = [N_{42}^e]^T = \iint_e \varepsilon_r (N_e)\frac{\partial (N_e)^T}{\partial y}\,dx\,dy,$$

$$[N_{34}^e] = [N_{43}^e]^T = \iint_e -\beta\varepsilon_r (N_e)(N_e)^T\,dx\,dy$$

$$[N_{44}] = \iint_e \varepsilon_r \left(\frac{\partial (N_e)}{\partial x}\frac{\partial (N_e)^T}{\partial x} + \frac{\partial (N_e)}{\partial y}\frac{\partial (N_e)^T}{\partial y} + \beta^2 (N_e)(N_e)^T\right) dx\,dy$$

$$[P] = [\mu_r]^{-1} = \begin{bmatrix} P_{XX} & P_{XY} & jP_{XZ} \\ P_{YX} & P_{YY} & jP_{YX} \\ -jP_{ZX} & -jP_{ZY} & P_{ZZ} \end{bmatrix}$$

$$[\mu_r] = \begin{bmatrix} \mu_X & 0 & 0 \\ 0 & \mu & -jk \\ 0 & jk & \mu \end{bmatrix} \quad \text{(Region A)} \tag{A1}$$

$$[\mu_r] = \begin{bmatrix} \mu_X & 0 & 0 \\ 0 & \mu & jk \\ 0 & -jk & \mu \end{bmatrix} \quad \text{(Region B and region C)} \tag{A2}$$

$$[\mu_r] = \begin{bmatrix} \mu & 0 & -jk \\ 0 & \mu_Y & 0 \\ jk & 0 & \mu \end{bmatrix} \quad \text{(Region P)} \tag{A3}$$

$$[\mu_r] = \begin{bmatrix} \frac{1}{4}\mu + \frac{3}{4}\mu_Y & \frac{\sqrt{3}}{4}(\mu - \mu_Y) & -\frac{1}{2}jk \\ \frac{\sqrt{3}}{4}(\mu - \mu_Y) & \frac{3}{4}\mu + \frac{2}{4}\mu_Y & -\frac{\sqrt{3}}{2}jk \\ \frac{1}{2}jk & \frac{\sqrt{3}}{2}jk & \mu \end{bmatrix}$$
(Region M) (A4)

$$[\mu_r] = \begin{bmatrix} \frac{1}{2}(\mu + \mu_Y) & \frac{1}{2}(\mu - \mu_Y) & -\frac{\sqrt{2}}{2}jk \\ \frac{1}{2}(\mu - \mu_Y) & \frac{1}{2}(\mu + \mu_Y) & -\frac{\sqrt{2}}{2}jk \\ \frac{\sqrt{2}}{2}jk & \frac{\sqrt{2}}{2}jk & \mu \end{bmatrix}$$
(Region N) (A5)

$$[\mu_r] = \begin{bmatrix} \frac{3}{4}\mu + \frac{1}{4}\mu_Y & \frac{\sqrt{3}}{4}(\mu - \mu_Y) & -\frac{\sqrt{3}}{2}jk \\ \frac{\sqrt{3}}{4}(\mu - \mu_Y) & \frac{1}{4}\mu + \frac{3}{4}\mu_Y & -\frac{1}{2}jk \\ \frac{\sqrt{3}}{2}jk & \frac{1}{2}jk & \mu \end{bmatrix}$$
(Region O) (A6)

$$\mu = \mu_d + (1 - \mu_d)\left\{\frac{M}{M_S}\right\}^{3/2}$$

$$\mu_X = \mu_Y = \mu_d\left(1 - (M/M)_S\right)^{5/2}$$

$$\mu_d = \frac{2}{3}\left[1 - \left(\frac{\gamma 4\pi M_S}{\omega}\right)^2\right]^{1/2} + \frac{1}{3}, \qquad k = \gamma 4\pi M/\omega.$$

$4\pi M_S$ is the saturated magnetization of the ferrite material and $4\pi M$ is the remanence magnetization of the ferrite. $\gamma = 2.8 \times 10^6$ Hz/Oe and ω is the operating frequency (in hertz).

ACKNOWLEDGMENT

The authors would like to acknowledge the discussions and help of Prof. Y. L. Chow, Department of Electronic Engineering, City University of Hong Kong, Kowloon, Hong Kong.

REFERENCES

[1] W. J. Ince, "Recent advances in diode and ferrite phaser technology for phased-array radars," *Microwave J.*, pp. 36–46, Sept. 1972.
[2] W. J. Ince and E. Stern, "Nonreciprocal remanence phase shifters in rectangular waveguide," *IEEE Trans. Microwave Theory Tech.*, vol. MTT-15, pp. 87–95, Feb. 1967.
[3] W. P. Clark, "A technique for improving the figure-of-merit of a twin-slab nonreciprocal ferrite phase shifter," *IEEE Trans. Microwave Theory Tech.*, vol. MTT-16, pp. 974–975, Nov. 1968.
[4] W. J. Ince, D. H. Temme, and F. G. Willwerth, "Toroid corner chamfering as a method of improving the figure of merit of latching ferrite phasers," *IEEE Trans. Microwave Theory Tech.*, vol. MTT-19, pp. 563–564, June 1971.
[5] W. Junding, "Analysis of transverse magnetization phase shifter of cross waveguide," in *Nat. Interchange Magn. Mater. Device Technol. Conf.*, Guanxian, Sichuan, China, Oct. 1977, pp. 1–8.
[6] A. Mizobuchi and H. Kurebayashi, "Nonreciprocal remanence ferrite phase shifter using grooved waveguide," *IEEE Trans. Microwave Theory Tech.*, vol. MTT-26, pp. 1012–1016, Dec. 1978.
[7] W. Che, W. Junding, K. Sha, and Y. Wen, "Phase-adjustment technique of the digital-latching ferrite phase shifter," *IEEE Trans. Microwave Theory Tech.*, vol. 47, pp. 1125–1127, July 1999.
[8] W. Che, E. K.-N. Yung, W. Junding, and K. Sha, "Improved design of broad-band latching ferrite phase shifter in a reduced-size grooved waveguide," *IEEE Trans. Microwave Theory Tech.*, vol. 49, pp. 727–730, Apr. 2001.
[9] B. Lax and K. T. Button, *Microwave Ferrites and Ferromagnetic*. New York: McGraw-Hill, 1962, pp. 379–382.
[10] E. Schlomann, "Theoretical analysis of twin slab phase shifters in rectangular waveguide," *IEEE Trans. Microwave Theory Tech.*, vol. MTT-14, pp. 15–23, Jan. 1966.
[11] J. Jin, *The Finite Element Method in Electromagnetic*. New York: Wiley, 1993.
[12] I. Bardi and O. Biro, "An efficient finite-element formulation without spurious modes for anisotropic waveguides," *IEEE Trans. Microwave Theory Tech.*, vol. 39, pp. 1133–1138, Dec. 1991.
[13] J. J. Green and F. Sandy, "Microwave characterization of partially magnetized ferrites," *IEEE Trans. Microwave Theory Tech.*, vol. MTT-22, pp. 641–645, June 1974.
[14] E. Schlomann, "Microwave behavior of partially magnetized ferrites," *J. Appl. Phys.*, vol. 41, no. 1, pp. 204–214, Jan. 1991.

Wenquan Che received the B.Sc. degree in electrical engineering from the East China Institute of Science and Technology, Nanjing, China, in 1990, the M.Sc. degree in electromagnetic field and microwave technology from the Nanjing University of Science and Technology, Nanjing, China, in 1995, and is currently working toward the Ph.D. degree at the City University of Hong Kong, Kowloon, Hong Kong.

From December 1999 to November 2000, she was a Research Assistant with the City University of Hong Kong. From March 1995 to November 1999, she was with the Nanjing University of Science and Technology, where she conducted teaching and research as a Lecturer in the areas of electromagnetic (EM) theory and microwave devices, especially ferrite devices. Her current research involves the development of waveguide-based ferrite devices in microwave frequency and planar/coplanar structure devices in millimeter-wave frequency for wireless communication.

Edward Kai-Ning Yung (M'85–SM'85) was born in Hong Kong. He received the B.Sc. degree in electrical engineering (with special distinction), and the M.Sc. and Ph.D. degrees from the University of Mississippi, University, in 1972, 1974, and 1977, respectively.

Upon graduation, he was briefly with the Electromagnetic Laboratory, University of Illinois at Urbana-Champaign. In 1978, he returned to Hong Kong and joined the Hong Kong Polytechnic. In 1984, he joined the newly established City University of Hong Kong, Kowloon, Hong Kong, where he was instrumental in setting up a new department. He was promoted to Full Professor in 1989, and in 1994, he was awarded one of the first two personal chairs in the University. He is the founding Director of the Wireless Communications Research Center (formerly known as the Telecommunications Research Center). He currently heads the Department of Electronic Engineering, which is the largest of its kind in Hong Kong with 220 full-time staff members, including 65 faculties. He has authored or co-authored over 120 journal papers and has presented 140 papers in international conferences. He is the External Examiner of numerous graduate students in sister universities, both local and overseas. He is also active in applied research, consultancy, and other types of technology transfers. Despite his heavy administrative load, he remains active in research in microwave devices and antenna designs for wireless communications. He is the principal investigator of many funded projects. He holds one patent. He is listed in *Who's Who in the World* and *Who's Who in Science and Engineering in the World*.

Prof. Yung is a Fellow of the Chinese Institution of Electronics, the Institution of Electrical Engineers (IEE), U.K., and the Hong Kong Institution of Engineers. He is a member of Eta Kappa Nu, Phi Kappa Phi, Tau Beta Pi, and the Electromagnetics Academy. He is also active in professional activities. He is currently the chairman of the electronics discipline of the Hong Kong Institution of Engineers. He has been the general chairman of many international conferences held in Hong Kong. He was the president of the Hong Kong Association for the Advancement of Science and Technology (1998–1999), president of the Association of Experts for the Modernization of China (1989–1990, 1998–1999), and vice president of the Hong Kong Institution of Engineers (1999–2000). He has been the recipient of numerous awards in applied research, including the 1991 Grand Prize in the Texas Instruments Incorporated Design Championship, the 1998 Silver Medal presented at the Chinese International Invention Exposition, and the 1999 CMA Design Award. He also co-authored a paper that won the 1996 Young Scientist Award presented at the International Symposium on Antennas and Propagation, Tokyo, Japan. He holds an honorary professorship with two major universities in China.

Suibing Chen received the B.S. degree in electronic engineering from the Institute of Northwest Telecommunication Engineering, Xian, China, in 1986, and the M.S. degree in electromagnetic field and microwave theory from the Nanjing University of Science and Technology, Nanjing, China, in 1998.

He is currently a Senior Engineer with the Department of Antenna and Feeding, East China Institute of Electronic Engineering, Hefei, China, where he conducts research in the areas of microwave devices in antenna and feed system.

Junding Wen received the B.Sc. degree in communication engineering from the Beijing Institution of Posts and Telecommunication, Beijing, China, in 1965.

From 1965 to 1985, he was engaged in the research of microwave transmission and radio equipment and microwave ferrite devices with the Nanjing Institute of Electronic Techniques. In 1985, he joined the Nanjing University of Science and Technology, Nanjing, China, as an Associate Professor, and in 1994, he became a Full Professor. His main interests include microwave ferrite theory, devices, and magnetostatic wave devices. He has authored or co-authored over 100 papers, mainly in refereed journals.